JOURNAL OF VIROLOGY, Dec. 1996, p. 8645–8652 Vol. 70, No. 12
0022-538X/96/$04.00+0

The Role of Gag in Human Immunodeficiency Virus Type 1 Virion Morphogenesis and Early Steps of the Viral Life Cycle

ALISE S. REICIN,[1] ASA OHAGEN,[2] LEI YIN,[1] STEFAN HOGLUND,[2] AND STEPHEN P. GOFF[3,4]*

Department of Medicine,[1] and Department of Biochemistry and Biophysics[3] and Howard Hughes Medical Institute,[4] College of Physicians and Surgeons, Columbia University, New York, New York 10032, and Department of Biochemistry[2] University of Uppsala, Uppsala, Sweden

Received 12 February 1996/Accepted 14 August 1996

The phenotypes of a series of mutant human immunodeficiency virus type 1 proviruses with linker insertion and deletion mutations within the *gag* coding region were characterized. These mutants, with mutations in the matrix, capsid, and p2 coding regions, produced replication-defective virion particles with defects in the early steps of the viral life cycle. To investigate this phenotype further, the abilities of mutant virion particles to enter T cells, initiate and complete reverse transcription, and transport the newly transcribed proviral DNA were investigated. Only 4 of 10 of the mutants appeared to make wild-type levels of viral DNA. Biochemical analyses of the mutants revealed the middle region of CA as being important in determining virion particle density and sedimentation in velocity gradients. This region also appears to be critical in determining the morphology of mature virion particles by electron microscopy. Particles with aberrant morphology were uninfectious, and only those mutants which displayed cone-shaped cores were capable of carrying out the early steps of the viral life cycle. Thus, the normal morphology of human immunodeficiency virus type 1 appears to be critical to infectivity.

The products of the human immunodeficiency virus type 1 (HIV-1) *gag* gene participate in many steps of the retroviral life cycle. The retroviral *gag* gene encodes the major structural proteins of the virion and is required for assembly and release of virion particles (8). Gag polyproteins can be assembled and released from cells as virion-like particles in the absence of other viral genes, suggesting that *gag* is the only viral gene essential for viral assembly (14, 17, 21, 28, 36–38). Nascent retroviral particles released from infected cells are composed of an immature core surrounded by a lipid bilayer. These particles are characterized by the presence of a doughnut-shaped structure in electron micrographs. The Gag proteins in these immature particles are still intact, but during and after budding from the cell surface, they are cleaved by the viral protease to generate the major internal proteins of the virion (termed MA, CA, NC, and p6). Gag processing in turn causes the doughnut structure to condense to an electron-dense cone-shaped core (12, 13, 46), attached to viral envelope by its narrow end (18). Although proteolytic processing is not a prerequisite for the formation of particles, it is absolutely essential for infectivity (16, 22, 30).

While it is clear that Gag proteins are essential for the formation and release of viral particles, these proteins have also been shown to play a role in the early steps of the viral life cycle (15, 20, 27, 35, 41, 44, 48). It is likely that the structure of the Gag proteins is important for viral entry, efficient virion disassembly and release of a transcriptase-active core, and the import of the preintegrative complex into the nucleus of the cell. While mutations throughout *gag* have been reported to block these early steps in the viral life cycle, Gag's mechanism of action in these steps has not been defined. It is possible that different regions of Gag play different roles in these early events.

We have previously reported the phenotypes of a series of HIV-1 Gag mutants containing linker insertion mutations (35). Of the 10 mutant proviruses, three did not make extracellular virion particles when transfected into COS7 cells. Two of these assembly-defective mutants had mutations in the C-terminal domain of CA. Seven of the mutant proviruses retained the ability to make, release, and process virion particles from COS7 cells. These particles contained the Env glycoprotein, viral genomic RNA, and the mature products of the Gag and Gag-Pol polyproteins, yet they were noninfectious or poorly infectious. The defect in these mutants appears to be in one of the early steps of the viral life cycle. To further understand the specific defect in these mutants, we have now examined their morphology by electron microscopy (EM) and biochemical means and have assayed their abilities to complete reverse transcription after infection and to transport the preintegrative complex to the nuclei of the infected cells. The N terminus and middle region of the CA protein appear to play a critical role in the production of mature virions with the correct morphology. In addition, only those mutants which displayed mature cone-shaped cores by EM were capable of carrying out the early steps of the viral life cycle. The morphology of the mature core appears to be critical for completion of the early steps prior to integration.

MATERIALS AND METHODS

Recombinant DNAs. The parent wild-type HIV-1 proviral DNA used in this study was plasmid R73/BH10 (generously provided by Mark Feinberg) (1). R73/BH10 contains the HXBc.2 provirus modified to be Vpu^+ and Nef^+ on a vector containing a simian virus 40 origin of replication. The resulting virus is Vpu^+, Nef^+, Vpr^-, and Vif^+. The construction of the linker insertions has been described previously (26, 35).

Cell culture, transfections, and infections. COS7 cells were maintained in Dulbecco's modified Eagle's medium supplemented with 10% fetal calf serum. Jurkat cells were maintained in RPMI 60 medium with 10% fetal calf serum. To generate virus stocks, COS7 cells were transfected with 1 to 5 μg of DNA per 2×10^6 to 4×10^6 cells by the chloroquine DEAE-dextran technique (7). Sixty hours posttransfection, culture supernatants were harvested and filtered through a 0.45-μm-pore-size filter. The virion particles were concentrated by centrifugation through a 25% sucrose cushion in TNE (10 mM Tris-HCl [pH 7.2], 10 mM NaCl, 1 mM EDTA) at 4°C for 2 h at 100,000 × *g*. The viral pellet was resuspended by incubation at 4°C overnight in 200 μl of medium containing 50 mM *N*-2-hydroxyethylpiperazine-*N*′-2-ethanesulfonic acid (HEPES; pH 7.0). The samples were normalized for reverse transcriptase (RT) activity and incubated at 37°C for 30

* Corresponding author. Phone: (212) 305-3794. Fax: (212) 305-8692.

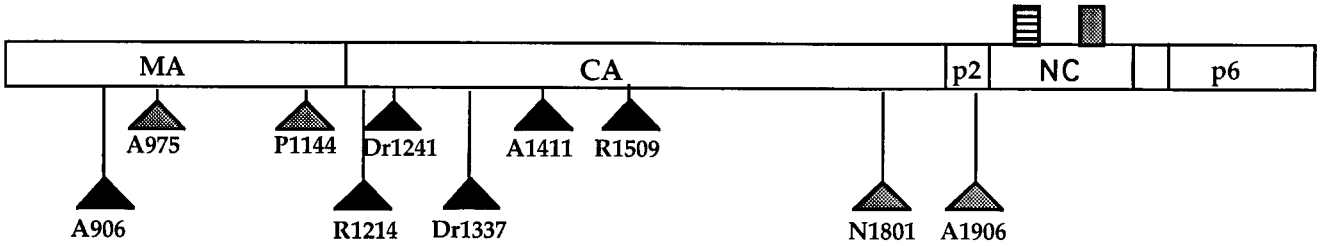

FIG. 1. Insertion mutations in HIV-1 *gag*. (A) The letter at the beginning of each mutant name indicates the restriction site used for linker insertion: A, *Alu*I; D, *Dde*I; Dr, *Dra*I; N, *Nla*IV, P, *Pvu*II; R, *Rsa*I. Numbers indicate the nucleotide position of the restriction site with respect to the 5′ edge of the 5′ LTR of the HIV-1 (HXBc.2) provirus. Black triangles represent noninfectious virions; grey triangles represent partially infectious virions; hatched boxes represent the two HIV NC Cys-His boxes.

min with 70 U of DNase I (Promega) in the presence of 10 mM $MgCl_2$ to remove contaminating transfected DNA. The DNase-treated virions were incubated for 2 h at 37°C with 6×10^6 Jurkat cells in 2 ml of medium containing Polybrene (0.8 μg/ml). The samples were then diluted 10-fold with fresh medium. To test for the spread of the virus throughout the cell culture, viral supernatants were harvested every 2 to 3 days and assayed for RT activity (32). For experiments involving PCR analysis of cells, 3×10^6 cells were removed 6 and 24 h after the addition of the fresh medium. The cells were washed in phosphate-buffered saline and lysed in PCR lysis buffer as described previously (43).

Assays for determining the assembly of particles in a single round in Jurkat cells were performed by transfecting the cells with 10 μg of DNA by a DEAE-dextran protocol as described previously (33). Forty-eight hours after transfection, culture supernatants were harvested and virion particles were purified as described above.

PCR analysis. DNA from 3.0×10^5 infected cells was subjected to PCR amplification under standard conditions, using primers corresponding to the U5 region of plus strand (nucleotides 9650 to 9669) and the R region of the minus strand (nucleotides 9591 to 9610) (5). Nucleotide positions of the oligonucleotide primers are according to the sequence of Ratner et al. (34). The PCR mixtures were subjected to 35 cycles with denaturation for 1 min at 94°C, primer annealing for 2 min at 65°C, extension for 3 min at 72°C, and a final 10-min extension step at 72°C. A portion of the amplified PCR products was subjected to gel electrophoresis, transferred to nitrocellulose, and probed with a α-^{32}P-labeled oligonucleotide containing HIV-specific sequences internal to the primer pairs. This analysis detects a 595-bp DNA fragment corresponding to the 2-long terminal repeat (LTR) junction of circular viral DNA (5).

EM. Suspensions of transfected COS7 cells and collected virus particles were fixed in freshly made 2.5% glutaraldehyde in phosphate-buffered saline and postfixed in 1% osmium tetroxide. After agar block enclosure and an additional treatment with 1% uranyl acetate, the cells were embedded in Epon. The sections were made approximately 60 to 80 nm thick to accommodate the volume of the core structure parallel to the section plane and poststained with an additional 1% uranyl acetate. Specimens were analyzed with a Zeiss CEM 902 electron microscope at an accelerating voltage of 80 kV. A liquid cooling trap of the specimen holder was used throughout.

Sucrose gradient analysis. For equilibrium density gradients, virions were concentrated from COS7-transfected supernatants as described above. The samples were spiked with Moloney murine leukemia virus (M-MuLV) particles collected from NIH 3T3 producer cell lines established by transfection with the full-length M-MuLV provirus pNCA (6) and were centrifuged through 20 to 60% continuous sucrose gradients (in phosphate-buffered saline) at 100,000 × *g* for 16 h in an SW41 rotor. Fractions were collected, and the density of each fraction was determined by weighing 100 μl of sucrose solution. The proteins in each fraction were then concentrated by the addition of trichloroacetic acid to a final concentration of 10%. The samples were than placed at −20°C for 10 min, centrifuged in a microcentrifuge for 10 min, and resuspended in Western loading buffer. Those fractions containing virion particles were identified by assaying for the presence of virion-associated Gag and RT proteins by Western blot (immunoblot) analysis using antiserum to HIV CA (p24), HIV RT (p66), and M-MuLV CA (p30) (35) and quantitated by use of a densitometer (Molecular Dynamics).

For nonequilibrium velocity gradients, purified HIV virions were layered on top of a 5 to 20% sucrose gradient and were centrifuged for 90 min at 20,000 × *g* in an SW41 rotor. Fractions were collected, and those containing virion particles were identified by assaying for RT activity as previously described (35) and quantitated by use of a PhosphorImager (Molecular Dynamics). These assays were repeated two to three times for each mutant.

Analysis of the detergent sensitivity of virion particles. Purified virions, harvested from COS7-transfected cultures, were resuspended in TNE and divided into two fractions. One fraction was incubated at 37°C for 30 min in the presence of 0.5% Triton X-100, and the other fraction was incubated in the absence of detergent. The samples were then centrifuged for 2 h at 100,000 × *g* over a 25% sucrose cushion containing the same detergent conditions as the 37°C incubation buffer. Pelleted virions were resuspended in Western loading buffer, boiled for 5 min, separated by electrophoresis on a sodium dodecyl sulfate (SDS)–12% polyacrylamide gel, transferred to nitrocellulose, and probed either with a mixture of monoclonal antisera to p24 and p17 (Dupont) or with an antiphosphotyrosine antibody (Transduction Laboratories, Lexington, Ky.) as recommended by the manufacturer. Nitrocellulose-bound proteins were immunodetected by enhanced chemiluminescence as previously described (25).

RESULTS

Positions of mutations in HIV-1 *gag* gene. To better define the roles of the various regions of Gag in virion morphogenesis and infectivity, we analyzed in further detail the morphological characteristics and the specific defect in replication of a series of assembly-competent, replication-defective Gag mutants. We previously described seven such linker insertion Gag mutants. Further studies identified an additional three mutants with linker insertion mutations in CA which were assembly competent in COS7 cells (data not shown). The location of each of the linker insertion mutants is shown in Fig. 1. The corresponding change in the amino acid sequence has previously been reported (26, 35). A906, A975, and P1144 contain linker insertion mutations in the MA domain of the *gag* coding region; R1214, Dr1241, Dr1337, A1411, R1509, and N1801 contain linker insertion mutations in CA. A1906 contains a linker insertion mutation in the p2 spacer peptide between CA and NC.

Virion assembly and release in Jurkat cells. The mutants were able to assemble and release particles in COS7 cells. To determine if these mutants were assembly competent in lymphoid cells, $CD4^+$ Jurkat cells were transfected with proviral

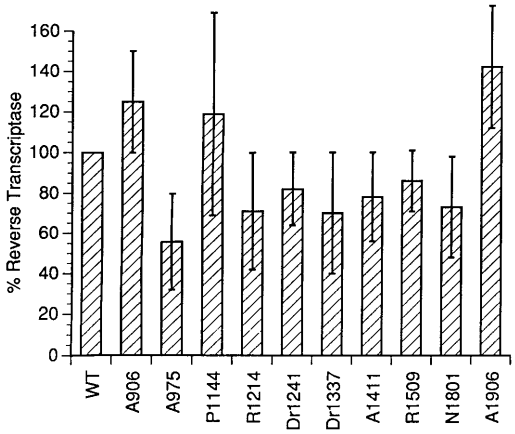

FIG. 2. Release of RT-containing virion particles from Jurkat cells transfected with Gag mutant proviruses. The virion-associated RT activity of each mutant is presented as a percentage of wild-type (WT) activity. The values given are the means of three transfections.

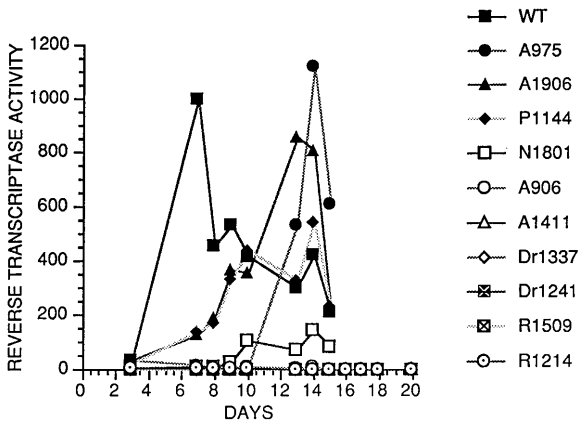

FIG. 3. Replication of the Gag linker insertion mutants in Jurkat cells. The cells were infected with normalized amounts of R73/BH10 (wild type [WT]) and mutant virion particles purified from COS7-transfected supernatants. The amounts of virion particles were normalized by RT activity. The infectivity was monitored as RT activity in the culture supernatant over time. Each RT value represents the amount of activity in 1.5 μl of culture supernatant.

DNA from each of the 10 mutants. Culture supernatants were harvested 48 and 72 h posttransfection, virions were concentrated and purified by pelleting over a sucrose cushion, and the presence of virion particles was assayed by analyzing the RT activity in each sample. We found comparable levels of both R73/BH10 and mutant virion particles in pelleted supernatants harvested at early times, suggesting that none of the mutants had a significant defect in the ability to assemble and release particles in Jurkat cells (Fig. 2). On day 2 posttransfection, the amounts of virion particles were nearly equivalent in the pelleted supernatants of all samples. However by day 3, R73/BH10 had two- to threefold more virion particles than many of the replication-defective mutants, implying that multiple rounds of infection had occurred (data not shown). The samples harvested on day 2 largely represent virion particle formation from the transfected cells.

Infectivity of the virions. To determine whether the mutant particles were infectious, Jurkat cells were incubated with wild-type or mutant virions which had been harvested and purified from COS7-transfected supernatants. Culture medium was harvested every 2 to 3 days and tested for virion-associated RT activity. These assays require viral spread to generate sufficient progeny virus to be detected by the RT assay. R73/BH10 induced the appearance of RT activity in culture supernatants by day 7 (Fig. 3). All 10 mutants had significant defects in viral infectivity. A906, R1214, Dr1241, A1411, Dr1337, and R1509 did not induce activity even when the cultures were tested to day 20, demonstrating that these mutants are all unconditionally noninfectious. The remaining four mutants, A975, P1144, N1801, and A1906, showed markedly delayed growth kinetics in Jurkat cells, with delays of 4 to 10 days relative to the wild type (Fig. 3). Preliminary analysis of the virus recovered from these assays suggested that at least two of the mutants, A975 and N1801, had reverted to generate infectious virus that replicated with wild-type kinetics (data not shown). In these revertants, analysis of the viral DNA showed retention of the original linker insertion, implying that a second-site suppressor mutation was responsible for the reversion. Further analysis of these revertants is ongoing.

Sucrose density and velocity gradients of Gag mutants. To further evaluate parameters dependent on the density, size, and shape of the mutant virions, sucrose density and velocity gradients of the Gag mutants were performed. Virion particles purified from COS7-transfected cells were spiked with M-MuLV and layered over 20 to 60% linear sucrose gradients. The M-MuLV served as an internal marker so that subtle differences in density could be determined. After equilibrium centrifugation, fractions were collected and the density was measured. The amount of virion particles in each fraction was determined by assaying for HIV- and MuLV-specific virion proteins in Western blot analyses. Wild-type HIV banded at a density slightly lighter than that of M-MuLV. The peak consistently appeared at a position approximately one-fourth fraction lighter than that of M-MuLV, corresponding to a density lighter by 0.002 g/ml. All of the mutant virions were very close to the density of the wild-type HIV-1 virions. Of the 10 mutants evaluated, those with mutations in MA, p2, and the very N terminus of CA had densities which were identical to or only slightly lighter than that of HIV; i.e., they appeared to peak 0 to 0.002 g/ml lighter than wild-type HIV (Table 1). However, four mutants with linker insertions in the amino-terminal half of CA had densities which were lighter than that of wild-type HIV by 0.003 to 0.005 g/ml (Table 1). These deviations in density from the wild-type level are very subtle and could be detected only with the use of M-MuLV as an internal marker in each gradient.

To assess the possibility of size or shape variation of the virion particles, nonequilibrium velocity gradients were performed. Purified virions were layered over 5 to 20% sucrose gradients and centrifuged for 90 min. Fractions were collected as described for the sucrose density gradients (representative plots are shown in Fig. 4). Mutants A906, A975, P1144, and R1214, with mutations in MA and the very N terminus of CA, appeared to peak at the same fractions as the wild type. In contrast, mutants Dr1241, Dr1337, A1411, R1509, N1801, and A1906 consistently appeared to sediment one to two fractions more slowly than the wild type, implying that these particles differed in size, mass, or shape from the wild type (Table 2). Differences in sedimentation rate are not proportional to differences in size for particles of uniform shape; small differences in sedimentation rate reflect larger differences in size. Thus, the mutant virions may be significantly smaller than wild-type virions or exhibit altered shape. No clear splaying of the curves was observed, as might have been expected if size heterogeneity had been present. These results were confirmed by using velocity gradients layered with mixtures of HIV and M-MuLV (data not shown).

Evaluation of the detergent sensitivity of virion particles. It has previously been shown that immature capsids which contain unprocessed $Pr55^{gag}$ and $Pr160^{gag\text{-}pol}$ are resistant to 0.5% Triton X-100, while mature viral capsids of HIV-1 (29), avian viruses (40, 42), and murine leukemia viruses (31, 47) are

TABLE 1. Densities of wild-type and mutant HIV

Sample	Δρ (g/ml ± 0.002) g/ml
A906	0.000
A975	−0.002
P1144	−0.002
R1214	0.000
Dr1241	−0.005
Dr1337	−0.003
A1411	−0.005
R1509	−0.005
N1801	0.000
A1906	0.000

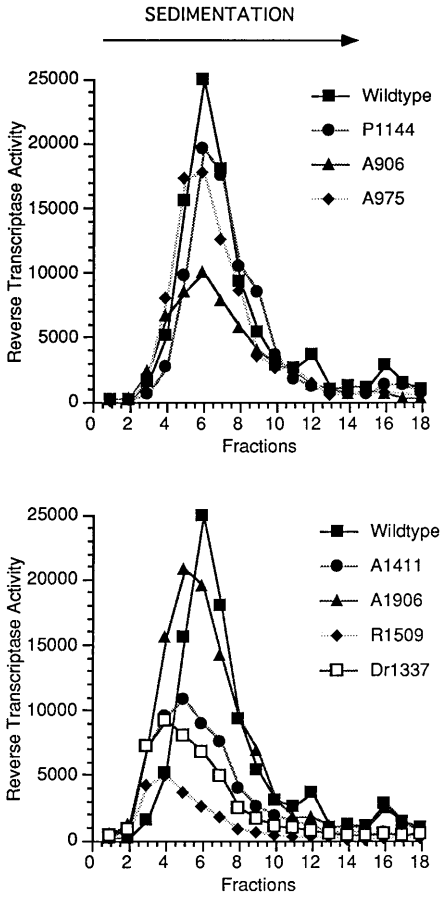

FIG. 4. Velocity gradient centrifugation of extracellular particles after transfection. Virion particles harvested from COS7-transfected culture media were analyzed by nonequilibrium centrifugation on 5 to 20% sucrose gradients. Individual fractions were analyzed for HIV virion content by RT assays. The top of the gradient is to the left, and the bottom of the gradient is to the right.

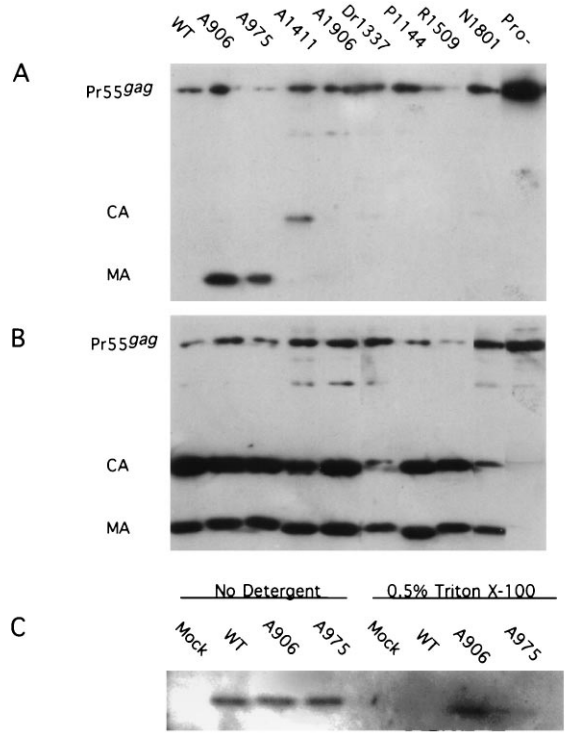

FIG. 5. Western blot of virion particles treated with detergent. COS7 cells were transfected with wild-type (WT) and mutant proviral DNA. Sixty hours posttransfection, virion particles were purified from the transfected-cell supernatant and the samples were split into two equal fractions. The fractions were incubated at 37°C with 0.5% Triton X-100 (A) or without detergent (B). The samples were then pelleted through a 25% sucrose cushion containing the same detergent conditions as the incubation buffer. Pelleted material was displayed on an SDS–12% polyacrylamide gel, transferred to nitrocellulose, and probed with a mixture of anti-p24 and anti-p17 antisera (A and B) or with an antiphosphotyrosine antibody (C).

disrupted under these detergent conditions. To determine whether the mutant virions had altered sensitivity to detergent, pelleted virions were incubated with or without 0.5% Triton X-100 and were recovered after centrifugation through a 25% sucrose cushion. Western immunoblotting was then performed on portions of the pelleted proteins. As a control, we analyzed the detergent sensitivity of the protease-defective mutant A2315, carrying a linker insertion in the protease coding region (26). As expected, the immature particles which contained uncleaved $Pr55^{gag}$ and $Pr160^{gag\text{-}pol}$ (data not shown) were preferentially pelleted in this protocol, while the mature cleavage products of $Pr55^{gag}$ and $Pr160^{gag\text{-}pol}$ were not (Fig. 5A). In samples treated without detergent, both cleaved and uncleaved Gag proteins were pelleted (Fig. 5B). The majority of the eight mutants tested appeared to have no change in their sensitivity to detergent.

TABLE 2. Velocity gradient centrifugation of wild-type and mutant HIV

Sample	Velocity (fraction of wild type value)
A906	1.00
A975	1.00
P1144	1.00
R1214	1.00
Dr1241	0.60
Dr1337	0.66
A1411	0.83
R1509	0.66
N1801	0.90
A1906	0.83

Three mutants, A1411, A906, and A975, showed altered phenotypes in this assay. After detergent treatment, A906 and A975 appeared to have MA as well as $Pr55^{gag}$ in the pelleted proteins; no mature CA was recovered. A906 had approximately two- to fourfold more MA pelleted after detergent treatment than did A975. Roughly 50% of the MA protein in mutant A906 and 15 to 20% of that in mutant A975 was pelleted after detergent treatment. These MA mutations appear to have changed the mature MA so that they form aggregates which do not include CA and are detergent resistant. Recent data suggest that a small fraction of MA is phosphorylated and that this phosphorylated protein appears to be associated with the preintegrative complex (11). To determine whether these mutant MA proteins were phosphorylated, the virion fractions which had not been detergent treated were analyzed by probing Western blots with an antiphosphotyrosine antibody. The level of phosphorylated MA in A906 and A975 was indistinguishable from the wild-type level (Fig. 5C). To analyze whether the detergent-resistant MA aggregates

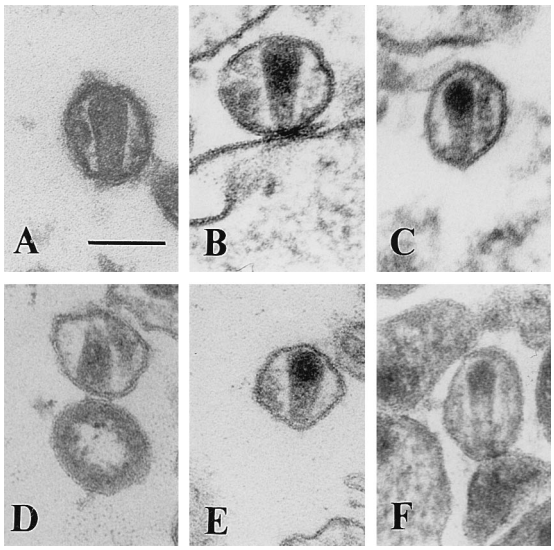

FIG. 6. Electron micrographs showing thin sections of wild-type and mutant virions. (A) Wild type; (B) A975; (C) P1144; (D) N1801; (E) A1906; (F) A906. The bar represents 100 nm.

contained phosphorylated MA proteins, Western blots of the fractions treated with detergent were probed as before (Fig. 5C). The detergent resistant aggregates contained phosphorylated MA, and the percentage of MA which was phosphorylated in these aggregates did not appear to differ from that of untreated virion-incorporated MA when normalized to the amount of MA present. Lastly, A1411 appears to have a low level of mature CA proteins which are resistant to detergent. This fraction appears to aggregate independently of MA.

EM analysis of mutants. To further examine the effects of the linker insertions on virion size and morphology, thin sections of transfected cells and virions were analyzed by transmission EM. Three hundred virion particles were visualized for each sample. Budding virion particles and extracellular immature and mature virion particles were detected in the wild-type specimen. The sizes of the wild-type particles varied between 90 and 160 nm. The structurally mature virus displayed an electron-dense, cone-shaped or round core, depending on the plane of sectioning (Fig. 6A). The narrow end of the cone-shaped structure was attached to the envelope by a core-envelope link as previously described (18). Mutants A975, P1144, N1801, and A1906 showed a virion morphology similar to the wild-type morphology, although the relative frequencies were altered (Fig. 6; Table 3). These mutants all appeared to have a 2- to 3.5-fold reduction in the proportion of mature cone-shaped virion particles. In addition, mutant A1906 showed a larger variation in size (70 to 210 nm) compared with the wild type.

The remainder of the mutants (A906, R1214, Dr1241, Dr1337, A1411, and R1509) showed no normal-appearing cone-shaped cores (Fig. 6F and 7). Cone-shaped or tubular cores were rarely detected in mutant A906; however, the conical core structures showed an irregular density compared with the wild-type cores (Fig. 6F; Table 3). These abnormal cores contained dense material in their broad end, and the material inside the narrow end appeared transparent. A similar core structure has been reported for *vif*-negative HIV-1 virions produced in nonpermissive cells. Some of the cone-shaped cores of the wild type and the A975, P1144, N1801, and A1906 mutants showed the same morphological appearance, but the percentage was much lower than that seen in A906 (data not shown).

The majority of the structurally mature particles of A906 exhibited a dense, round core structure. This morphology was exhibited by all of the mature particles of R1214, Dr1241, Dr1337, A1411, and R1509 (Fig. 7). In addition, like mutant A1906, mutants A1411 and R1509 were heterogeneous in size, with diameters varying between 80 and 240 nm. Additionally, some particles produced by COS7 cells transfected with Dr1241, Dr1337, and A1411 showed an increase in the thickness of the viral envelope and occasionally revealed an electron-dense layer directly underneath the plasma membrane.

Analysis of early steps of the viral life cycle. To identify the step in the viral life cycle affected by the mutations, wild-type and mutant virions harvested from COS7-transfected supernatants were used to acutely infect Jurkat cells. At 6 and 24 h after infection, the cells were harvested and total cellular DNA was isolated. This DNA was then subjected to PCR amplification using primers which span the U3/U5 junction present in circular two-LTR forms of viral DNA. Circular forms of the retroviral genome containing one and two LTRs are found in the nuclei of newly infected cells only after the synthesis of linear viral DNA and its transport to the nucleus (4). Although the circular forms of viral DNA are not preintegration precursors (4), the presence of DNA which is amplified by primers spanning the U3/U5 junction serves as a marker of viral DNA synthesis and its transport to the nucleus of the infected cell. In addition, since the U3/U5 junction does not exist in the plasmid proviral DNA used in the initial COS7 transfection, use of primers which span this junction ensures that amplified DNA does not represent contaminating input plasmid DNA. DNA harvested from T cells infected with A906, R1214, Dr1241, A1411, Dr1337, and R1509 failed to amplify any viral DNA with these primers (Fig. 8), implying that the defect in these mutants is quite early in the viral life cycle. The defect could be in uncoating of the virion particles, before any reverse transcription occurs, or in movement into the nucleus, before circular forms can be made. Mutants A975, P1144, N1801, and A1906, however, had detectable levels of newly transcribed circular DNA (Fig. 8). These analyses were repeated three to five times for each sample. Mutant A1906 consistently displayed levels of DNA which were greater than or almost equivalent to wild-type levels. A975, P1144, and N1801 displayed a 2- to 10-fold reduction in the levels of amplified DNA, depending on the experiment. It is not clear how faithfully these levels of PCR products correlate with the actual levels of circular

TABLE 3. Quantitative analysis of virus core morphology of wild-type and mutant particles produced in COS7 cells[a]

Virus	% Mature particles with cone-shaped core	% Particles with round, dense central core structure	% Immature particles or budding structures	% Other
Wild type	31	37	30	2
A906	2	47	44	7
A975	10	40	45	5
P1144	19	27	42	12
R1214	0	25	72	3
Dr1241	0	47	49	4
Dr1337	0	60	32	8
A1411	0	42	55	3
R1509	0	62	30	8
N1801	15	40	40	5
A1906	9	45	39	7

[a] Three hundred virions were analyzed for each sample.

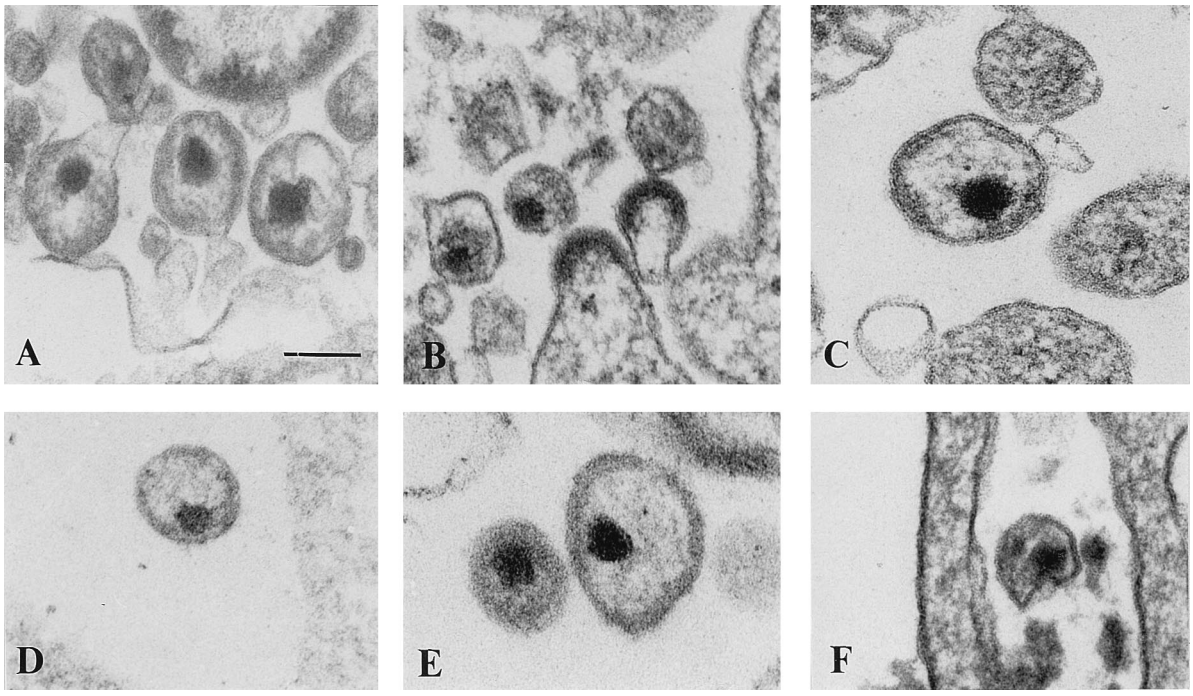

FIG. 7. Electron micrographs showing thin sections of mutant virions. (A) A906; (B) R1214; (C) Dr1241; (D) Dr1337; (E) A1411; (F) R1509. The bar represents 100 nm.

viral DNA present in the cells, but it is clear that these mutants are capable of carrying out these steps.

When the results of the EM analyses were compared with the data on the ability of the mutants to carry out the early steps in infection, a direct correlation was found. Those mutants which had no detectable particles with normal-appearing cone-shaped cores were defective in the very early steps of the virion life cycle. Conversely, the four mutants which had virion particles with normal morphology were capable of making circular two-LTR DNA (Table 4). These results imply that the normal packing of the cone-shaped core is essential for efficient transit through the early stages of viral replication.

DISCUSSION

We have characterized the phenotypes of a panel of linker insertion mutations in the *gag* coding region. These mutants were all assembly competent in COS7 cells as well as in $CD4^+$ T cells, but they were all replication defective. The mutants can be divided into different phenotypic groups.

Mutants R1214, Dr1241, Dr1337, A1411, and R1509 have linker insertions in the N-terminal half of the CA protein. These mutants were noninfectious, were unable to carry out the early steps in the viral life cycle, and appeared to make mature virion particles which were morphologically abnormal by EM as well as by biochemical tests. Particles produced by these mutants had dense, circular, eccentrically located cores instead of cone-shaped cores. These mutants also displayed various abnormalities in size both by EM and by sedimentation. Mutants Dr1241, Dr1337, A1411, and R1509 appeared to sediment more slowly than the wild type in velocity gradients, and A1411 and R1509 displayed size heterogeneity, as judged by EM. After detergent treatment, mutant A1411 appeared to contain CA aggregates which were resistant to the detergent conditions which disrupted wild-type mature virions. Lastly, the densities of Dr1241, Dr1337, A1411, and R1509 as deter-

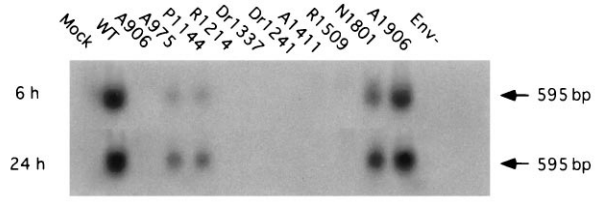

FIG. 8. PCR analysis of circular viral DNA. Jurkat cells were infected with wild-type (WT) and mutant virions. At 6 and 24 h postinfection, DNA was isolated from the infected cells and subjected to PCR and to Southern analysis as described in the text. The position of the 595-bp fragment hybridizing to the probe is indicated.

TABLE 4. Correlation between virion morphology and the ability to make circular two-LTR viral DNA after infection

Virus	% Mature particles with dense, cone-shaped core	Ability to carry out early steps in the viral life cycle[a]
Wild type	31	++
A906	0	−
A975	9	+
P1144	9	+
R1214	0	−
Dr1241	0	−
Dr1337	0	−
A1411	0	−
R1509	0	−
N1801	15	−
A1901	9	++

[a] ++, wild-type level of two-LTR viral DNA; +, 2- to 10-fold reduction in levels of two-LTR viral DNA; −, no two-LTR viral DNA.

mined by sucrose density centrifugation were slightly lighter than that of wild-type HIV. These results imply that the N-terminal and middle portions of CA are critical in the formation of morphologically normal virions. The region is important in formation of the cone-shaped cores and may play some role, directly or indirectly, in determining the size and density of the particles. Deletions in the major homology region of CA as well as a deletion of the C terminus of CA and the N terminus of NC have previously been shown to result in virion particles with much more dramatically altered densities (approximately 0.02 g/ml lighter than wild-type particles) (2, 39). It is noteworthy that only those mutants containing mutations outside the N-terminal and middle portions of CA had any evidence of cone-shaped cores; those mutants containing linker insertions within this region did not. These results are consistent with those previously published for HIV-1 CA deletion mutants (9) and Rous sarcoma virus CA deletion mutants (45).

Mutant A906, with a linker mutation in the MA domain of Gag, was also noninfectious and unable to carry out the early steps of the virion life cycle. This mutant did appear to have a few particles with cone-shaped cores, but the majority of these particles displayed nonhomogeneous packing of the core instead of the normal electron-dense, cone-shaped core structure. The morphological appearance was similar to that reported for *vif*-negative virions produced in nonpermissive cells (19). Mutant A906 and its parent, R73/BH10, are *vif*$^+$. In addition, the COS7 cells used to produce the virion particles are permissive, and therefore even *vif*-negative virus produced in these cells has a wild-type morphology (19). Despite this, virions produced in COS7 cells transfected with mutant A906 had only a few cone-shaped cores. This finding may suggest that MA is important in mediating the action of Vif and its putative cellular counterpart in the packing of the core structure. Given the recent report that Vif is packaged into virions and is associated with viral core structures (24), it is possible that core-associated MA plays a role in the packaging of Vif into the core.

Mutants N1801 and A1906 both had cone-shaped cores and were able to carry out the early steps in the virion life cycle. However, mutant N1801 with a linker insertion in the C terminus of CA sedimented slightly more slowly than the wild type in velocity gradients, and A1906, with a linker insertion in the p2 domain of Gag, displayed size heterogeneity by EM and sedimented more slowly than the wild type in velocity gradients. The size heterogeneity seen with A1906 is similar to but much less drastic than those reported for mutants which lack the entire p2 spacer peptide (23), which confirms that this region is important in virion morphogenesis. It appears that the formation of the cone-shaped core and the ability to carry out the early steps in the virion life cycle are distinct from the ability of the virus to form particles with wild-type size distribution.

Mutants A975, P1144, N1801, and A1906 all displayed virion particles with uniformly packaged cone-shaped cores. These four mutants were the only ones of those evaluated which were able to initiate and complete reverse transcription and transport the proviral DNA to the nucleus of the infected cell. Although these mutants were able to carry out these early steps, they were defective in infectivity. It is possible that these mutants have an impaired ability to integrate proviral DNA into the host chromosome. It is also possible that the defect in infectivity represents a combination of partial defects. Mutant P1144 had detectable but decreased levels of newly reverse-transcribed circular DNA. Similarly, a 13-amino-acid deletion at the N terminus of MA which overlaps the region of the P1144 linker insertion has been shown to be defective in viral DNA synthesis after infection (48). A stretch of highly conserved amino acids in this region (AADTGHSSQV; residues 118 to 127) shows homology to a similar sequence in the VP1 region of poliovirus (3). In poliovirus, this region has been implicated in the process of virus penetration (10). It is possible that because of a partial defect in entry, viral DNA synthesis is reduced.

The exact step which is blocked in those mutants unable to carry out the early steps of the virion life cycle remains unknown. It is unclear whether the defect is in the initiation or completion of reverse transcription or in the transport of the newly transcribed DNA to the nucleus of the infected cell. Our belief is that the defect is in uncoating. We suppose that the abnormal core morphology manifested by these mutants blocks the structural changes which are critical for postentry intracellular steps. Further analyses will be necessary to determine the exact defect in these mutants.

ACKNOWLEDGMENTS

This work was supported in part by grant AI 24845 from the National Institute of Allergy and Infectious Diseases to S.P.G. A.S.R. was an Aaron Diamond Foundation Young Faculty Awardee and an Investigator of the American Heart Association. S.P.G. is an Investigator of the Howard Hughes Medical Institute. This work was supported by the Swedish Medical Research Council (A.O. and S.H.).

REFERENCES

1. **Aldovini, A., and M. B. Feinberg.** 1990. Transfection of molecularly cloned HIV genomes, p. 166. *In* A. Aldovini and B. D. Walker (ed.), Techniques in HIV research. Stockton Press, New York.
2. **Bennett, R. P., T. D. Nelle, and J. W. Wills.** 1993. Functional chimeras of the Rous sarcoma virus and human immunodeficiency virus Gag proteins. J. Virol. **67:**6487–6498.
3. **Bloomberg, J., and P. Medstrand.** 1990. A sequence in the carboxy terminus of the HIV-1 matrix protein is highly similar to sequences in membrane-associated proteins of other RNA viruses: possible functional implications. New Biol. **2:**1044–1046.
4. **Brown, P. O., B. Bowerman, H. E. Varmus, and J. M. Bishop.** 1987. Correct integration of retroviral DNA in vitro. Cell **49:**347–356.
5. **Bukrinsky, M. I., S. Haggerty, M. P. Dempsey, N. Sharova, A. Adzhubei, L. Spitz, P. Lewis, D. Goldfarb, M. Emerman, and M. Stevenson.** 1993. A nuclear localization signal within HIV-1 matrix protein that governs infection of non-dividing cells. Nature (London) **365:**666–669.
6. **Colicelli, J., and S. P. Goff.** 1988. Sequence and spacing requirements of a retrovirus integration site. J. Mol. Biol. **199:**47–50.
7. **Cullen, B.** 1987. Use of eukaryotic expression technology in the functional analysis of cloned genes. Methods Enzymol. **152:**684–704.
8. **Dickson, C., R. Eisenman, H. Fan, E. Hunter, and N. Teich.** 1984. Protein biosynthesis and assembly, p. 513–648. *In* R. Weiss, N. Teich, H. Varmus, and J. Coffin (ed.), RNA tumor viruses, vol. 1. Cold Spring Harbor Laboratory, Cold Spring Harbor, N.Y.
9. **Dorfman, T., A. Bukovsky, A. Ohagen, S. Hoglund, and H. Gottlinger.** 1994. Functional domains of the capsid protein of human immunodeficiency virus type 1. J. Virol. **68:**8180–8187.
10. **Fricks, C. E., and J. M. Hogle.** 1990. Cell-induced conformational change in poliovirus: externalization of the amino terminus of VP1 is responsible for liposome binding. J. Virol. **64:**1934–1945.
11. **Gallay, P., S. Swingler, J. Song, F. Bushman, and D. Trono.** 1995. HIV nuclear import is governed by the phosphotyrosine-mediated binding of matrix to the core domain of integrase. Cell **83:**569–576.
12. **Gelderblom, H. R.** 1991. Assembly and morphology of HIV: potential effect of structure on viral function. AIDS **5:**617–638.
13. **Gelderblom, H. R., E. H. Hausmann, M. Ozel, G. Pauli, and M. A. Koch.** 1987. Fine structure of the human immunodeficiency virus (HIV) and immunolocalization of structural proteins. Virology **156:**171–176.
14. **Gheysen, D., E. Jacobs, F. deForesta, C. Thiriart, M. Francotte, D. Thines, and M. De Wilde.** 1989. Assembly and release of HIV-1 precursor Pr55^{gag} virus-like particles from recombinant baculovirus infected insect cells. Cell **59:**103–112.
15. **Gorelick, R. J., S. M. Nigida, J. R. Bess, L. O. Arthur, L. E. Henderson, and A. Rein.** 1990. Noninfectious human immunodeficiency virus type 1 mutants deficient in genomic RNA. J. Virol. **64:**3207–3211.
16. **Gottlinger, H. G., J. G. Sodroski, and W. A. Haseltine.** 1989. Role of capsid precursor processing and myristoylation in morphogenesis and infectivity of

human immunodeficiency virus type 1. Proc. Natl. Acad. Sci. USA **86:**5781–5785.
17. **Haffar, O., J. Garrigues, B. Travis, P. Moran, J. Zarling, and S.-L. Hu.** 1990. Human immunodeficiency virus-like, nonreplicating, *gag-env* particles assemble in a recombinant vaccinia virus expression system. J. Virol. **64:**2653–2659.
18. **Hoglund, S., L. G. Ofverstedt, A. Nilsson, P. Lundquist, H. Gelderbloom, M. Ozel, and U. Skolund.** 1992. Spatial visualization of the maturing HIV-1 core and its linkage to the envelope. AIDS Res. Hum. Retroviruses **8:**1–7.
19. **Hoglund, S., A. Ohoagen, K. Lawrence, and D. Gabzuda.** 1994. Role of *vif* during packing of the core of HIV-1. Virology **201:**349–355.
20. **Hsu, H.-W., P. Schwartzberg, and S. Goff.** 1985. Point mutations in the P30 domain of the *gag* gene of the Moloney murine leukemia virus. Virology **142:**211–214.
21. **Karacostas, V., K. Nagashima, M. A. Gonda, and B. Moss.** 1989. Human immunodeficiency virus-like particles produced by a vaccinia expression vector. Proc. Natl. Acad. Sci. USA **86:**8964–8967.
22. **Kohl, N. E., E. A. Emini, W. A. Schleif, L. J. Davis, J. C. Heimbach, R. A. Dixon, E. M. Scolnick, and I. S. Sigal.** 1988. Active human immunodeficiency virus protease is required for viral infectivity. Proc. Natl. Acad. Sci. USA **85:**4686–4690.
23. **Krausslich, H.-G., M. Facke, A.-M. Heuser, J. Konvalinka, and H. Zentgraf.** 1995. The spacer peptide between human immunodeficiency virus capsid and nucleocapsid proteins is essential for ordered assembly and viral infectivity. J. Virol. **69:**3407–3419.
24. **Liu, H., X. Wu, M. Newman, G. Shaw, B. H. Hahn, and J. C. Kappes.** 1995. The vif protein of human and simian immunodeficiency viruses is packaged into virions and associated with viral core structures. J. Virol. **69:**7630–7638.
25. **Luban, J., K. L. Bossolt, E. K. Franke, G. V. Kalpana, and S. P. Goff.** 1993. Human immunodeficiency virus type 1 gag protein binds to cyclophilins A and B. Cell **73:**1067–1078.
26. **Luban, J., C. Lee, and S. P. Goff.** 1993. Effect of linker insertion mutations in the human immunodeficiency virus type 1 *gag* gene on activation of viral protease expressed in bacteria. J. Virol. **67:**3630–3634.
27. **Mammano, F., A. Ohagen, S. Hoglund, and H. G. Gottlinger.** 1994. Role of the major homology region of human immunodeficiency virus type 1 in virion morphogenesis. J. Virol. **68:**4927–4936.
28. **Mergener, K., M. Facke, R. Welker, V. Brinkmann, H. R. Gelderblom, and H. G. Krausslich.** 1992. Analysis of HIV particle formation using transient expression of subviral constructs in mammalian cells. Virology **186:**25–39.
29. **Park, J., and C. D. Morrow.** 1993. Mutations in the protease gene of human immunodeficiency virus type 1 affect release and stability of virus particles. Virology **194:**843–850.
30. **Peng, C., B. K. Ho, T. W. Chang, and N. T. Chang.** 1989. Role of human immunodeficiency virus type 1-specific protease in core protein maturation and viral infectivity. J. Virol. **63:**2550–2556.
31. **Pepinsky, R. B.** 1983. Localization of lipid-protein and protein-protein interactions within the murine retrovirus gag precursor by a novel peptide-mapping technique. J. Biol. Chem. **258:**11229–11235.
32. **Prasad, V. R., I. Lowy, T. De Los Santos, L. Chiang, and S. P. Goff.** 1991. Isolation and characterization of a dideoxyguanosine triphosphate-resistant mutant of human immunodeficiency virus reverse transcriptase. Proc. Natl. Acad. Sci. USA **88:**11363–11367.
33. **Queen, C., and D. Baltimore.** 1983. Immunoglobulin gene transcription is activated by downstream sequence elements. Cell **33:**741–748.
34. **Ratner, L., W. Haseltine, R. Patarca, K. J. Livak, B. Starcich, S. F. Joseph, E. R. Doran, J. A. Rafalski, E. A. Whitwhoen, K. Baumeister, L. Ivanofff, S. R. Petteway, M. L. Pearson, J. A. Lautenberg, T. S. Papas, J. Ghrayeb, N. T. Chang, R. C. Gallo, and F. Wong-Staal.** 1985. Complete nucleotide sequence off the AIDS virus, HTLV-III. Nature (London) **313:**277–284.
35. **Reicin, A., S. Paik, R. Berkowitz, J. Luban, I. Lowy, and S. Goff.** 1995. Linker insertion mutations in the human immunodeficiency virus type 1 *gag* gene: effects on virion particle assembly, release, and infectivity. J. Virol. **69:**642–650.
36. **Royer, M., S. S. Hong, B. Gay, M. Cerutti, and P. Boulanger.** 1992. Expression and extracellular release of human immunodeficiency virus type 1 Gag precursors by recombinant baculovirus-infected cells. J. Virol. **66:**3230–3235.
37. **Shioda, A. J., M.-I. Cho, M.-L. Hammarskjold, and D. Rekosh.** 1990. Production of human immunodeficiency virus (HIV)-like particles from cells infected with recombinant vaccinia viruses carrying the *gag* gene of HIV. Virology **175:**139–148.
38. **Smith, A. J., M.-I. Cho, M.-L. Hammarskjold, and D. Rekosh.** 1990. Human immunodeficiency virus type 1 $Pr55^{gag}$ and $Pr160^{gag\text{-}pol}$ expressed from a simian virus 40 late replacement vector are efficiently processed and assembled into virus-like particles. J. Virol. **64:**2743–2750.
39. **Srinivasakumar, N., M.-L. Hammarskjold, and D. Rekosh.** 1995. Characterization of deletion mutants in the capsid region of human immunodeficiency virus type 1 that affect particle formation and Gag-Pol precursor incorporation. J. Virol. **69:**6106–6114.
40. **Stewart, L., G. Schatz, and V. M. Vogt.** 1990. Properties of avian retrovirus particles defective in viral protease. J. Virol. **64:**5076–5092.
41. **Strambio-de-Castillia, C., and E. Hunter.** 1992. Mutational analysis of the major homology region of Mason-Pfizer monkey virus by use of saturation mutagenesis. J. Virol. **66:**7021–7032.
42. **Stromberg, K., N. E. Hurley, N. L. Davis, R. R. Rueckert, and E. Fleissner.** 1974. Structural studies of avian myeloblastosis virus: comparison of polypeptides in virion and core component by sodium dodecyl sulfate-polyacrylamide gel electrophoresis. J. Virol. **13:**513–528.
43. **von Schwedler, U., J. Song, C. Aiken, and D. Trono.** 1993. *vif* is crucial for human immunodeficiency virus type 3 proviral DNA synthesis in infected cells. J. Virol. **67:**4945–4955.
44. **Wang, C.-T., and E. Barklis.** 1993. Assembly, processing, and infectivity of human immunodeficiency virus type 1 Gag mutants. J. Virol. **67:**4264–4273.
45. **Weldon, R. A. J., and J. W. Wills.** 1993. Characterization of a small (25-kilodalton) derivative of the Rous sarcoma virus Gag protein competent for particle release. J. Virol. **67:**5550–5561.
46. **Wills, J. W., and R. C. Craven.** 1991. Form, function, and use of retroviral Gag proteins. AIDS **5:**639–654.
47. **Yoshinaka, Y., and R. B. Luftig.** 1977. Murine leukemia virus morphogenesis: cleavage of P70 in vitro can be accompanied by a shift from a concentrically coiled internal strand ("immature") to a collapsed ("mature") form of the virus core. Proc. Natl. Acad. Sci. USA **74:**3446–3450.
48. **Yu, X., Q. C. Yu, T. H. Lee and M. Essex.** 1992. The C terminus of human immunodeficiency virus type 1 matrix protein is involved in early steps of the virus life cycle. J. Virol. **66:**5667–5670.